Catalyzed β scission of a carbenium ion III — Scission observed in ab initio molecular dynamics simulations

Greg M. Berner and Allan L. L. East

Abstract: The β scission (cracking) of branched carbenium ions have been observed in molecular dynamics simulations, possibly for the first time. Simulations were performed with molecular dynamics based on PW91 density functional theory, and which included three-dimensional periodic boundary replication of the unit cell to mimic long-range bulk effects. A rising-temperature algorithm was used to encourage reaction within the narrow time windows ($\sim$10 ps) of the simulations. Twenty-eight simulations were performed, featuring alkyl ions in three different catalytic systems: the ionic liquid, $[(C_5H_5NH^+)_5(Al_2Cl_7^-)_6]^-$, the chabazite zeolite, $[AlSi_{23}O_{48}]^-$, and the chabazite zeolite, $[Al_4Si_{20}O_{45}(OH)_3]^-$. Twenty-four runs began with unbranched *sec-n*-alkyl ions, but only one exhibited β scission, and only after branching to a tertiary ion and under extreme heating. In contrast, the four simulations that began with branched alkyl ions were all successful in demonstrating β scission at lower temperatures: 2,4,4-trimethyl-2-pentyl ion and 2,4-dimethyl-2-hexyl ion in each of the first two catalysts. The lifetimes of desorbed alkyl ions in the chabazite models were < 5 ps at 1000–1500 K. The β scission results support the classical Weitkamp et al. (*Appl. Catal.* **1983,** *8,* 123) mechanism over the nonclassical Sie (*Ind. Eng. Chem. Res.* **1992,** *31,* 1881) and the chemisorping Kazansky et al. (*J. Catal.* **1989,** *119,* 108) mechanisms.

Key words: C–C bond fission, cationic β scission, carbenium ions, alkyl ions, protonated cyclopropane (PCP^+), catalysis, chloroaluminate, catalytic cracking mechanism.

Résumé : On a observé, peut être pour la première fois, une scission β (craquage) d'ions carbénium ramifiés dans des simulations de dynamique moléculaire. Les simulations ont été effectuées à l'aide de la dynamique moléculaire basée sur la théorie de la fonctionnelle de densité PW91 qui inclut une réplication tridimensionnelle de la frontière périodique de la cellule unitaire pour représenter les effets globaux à long terme. On a utilisé un algorithme avec température croissante pour encourager la réaction vers des fenêtres étroites de temps ($\sim$10 ps) des simulations. On a effectué vingt-huit simulations mettant en évidence des ions alkyles dans trois systèmes catalytiques différents, un liquide ionique, $[C_5H_5NH^+)_5(Al_2Cl_7^-)_6]^-$, la chabazite zéolithe, $[AlSi_{23}O_{48}]^-$ et la zéolithe chabazite, $[Al_4Si_{20}O_{45}(OH)_3]^-$. Vingt-quatre de ces simulations commençaient avec des ions linéaires alkyles secondaires, mais seulement un a présenté une scission β et uniquement après avoir ramifié la chaîne vers un ion tertiaire, avec un chauffage intense. Par ailleurs, les quatre simulations lancées avec des ions ramifiés ont toutes conduit à des scissions β, à des températures plus basses, dont l'ion 2,4,4-triméthylpent-2-yle et l'ion 2,4-diméthylhex-2-yle dans chacun des deux premiers catalyseurs. Les temps de vie des ions alkyles désorbés dans les modèles de la chabazite sont de < 5 ps à 1000–1500 K. Les résultats de scission β sont en accord avec le mécanisme classique de Weitkamp et al. (*Appl. Catal.* **1983,** *8,* 123) concernant le mécanisme non classique de Sie (*Ind. Eng. Chem. Res.* **1992,** *31,* 1881) et celui de chimisorption de Kazansky et al. (*J. Catal.* **1989,** *119,* 108).

Mots-clés : fission d'une liaison C–C, scission cationique β, ions carbénium, ions alkyles, PCP^+, catalyse, chloroaluminate, mécanisme de craquage catalytique.

[Traduit par la Rédaction]

Introduction

In petroleum cracking of aliphatic hydrocarbon feedstock, the dominant C–C-bond scission step is β scission of carbocations (carbenium ions). The 1949 mechanisms of Thomas[1] and Greensfelder et al.[2] assumed classical alkyl ions with a three-coordinate charged carbon atom and viewed primary carbocations as acceptable primary products of the scission. In the ensuing 60 years, primary carbocations have proven to be impossibly recalcitrant to observation, and in response to this "primary carbocation dilemma", several modern versions of the β scission mechanism have been proposed. Review articles in 2001[3] and 2007[4] have expressed chagrin that the proper mechanism has still not been resolved. In this paper, we address this problem by reporting the results of ab initio molecular dynamics simulations, which shed light on which of these proposals is most likely to be correct.

In 1983, Weitkamp, Jacobs, and Martens (WJM)[5] proposed a mechanism variation (Fig. 1, top) that kept the concept of classical carbocations, but avoided the formation of

Received 21 February 2009. Accepted 18 June 2009. Published on the NRC Research Press Web site at canjchem.nrc.ca on 8 October 2009.

This article is part of a Special Issue dedicated to Professor T. Ziegler.

G.M. Berner and A.L.L. East.[1] Department of Chemistry and Biochemistry, University of Regina, Regina, SK S4S 0A2, Canada.

[1]Corresponding author (e-mail: Allan.East@uregina.ca).

Fig. 1. Three commonly cited mechanisms for catalytic β scission. Upper: Weitkamp, Jacobs, and Martens classical mechanism,[5] where *m* is the minimum number of carbons needed in the alkyl ion. Middle: Sie PCP$^+$ mechanism.[6] Lower: Li and East's version[14] of Kazansky and Senchenya[10] and van Santen and co-workers[11] chemisorption mechanism, where A, B, and C are the electron rearrangement steps, which could be stepwise or concerted. The extra final step of hydride transfer in the Sie mechanism,[6] presumably from another alkane in a chain reaction, would be common to all three mechanisms.

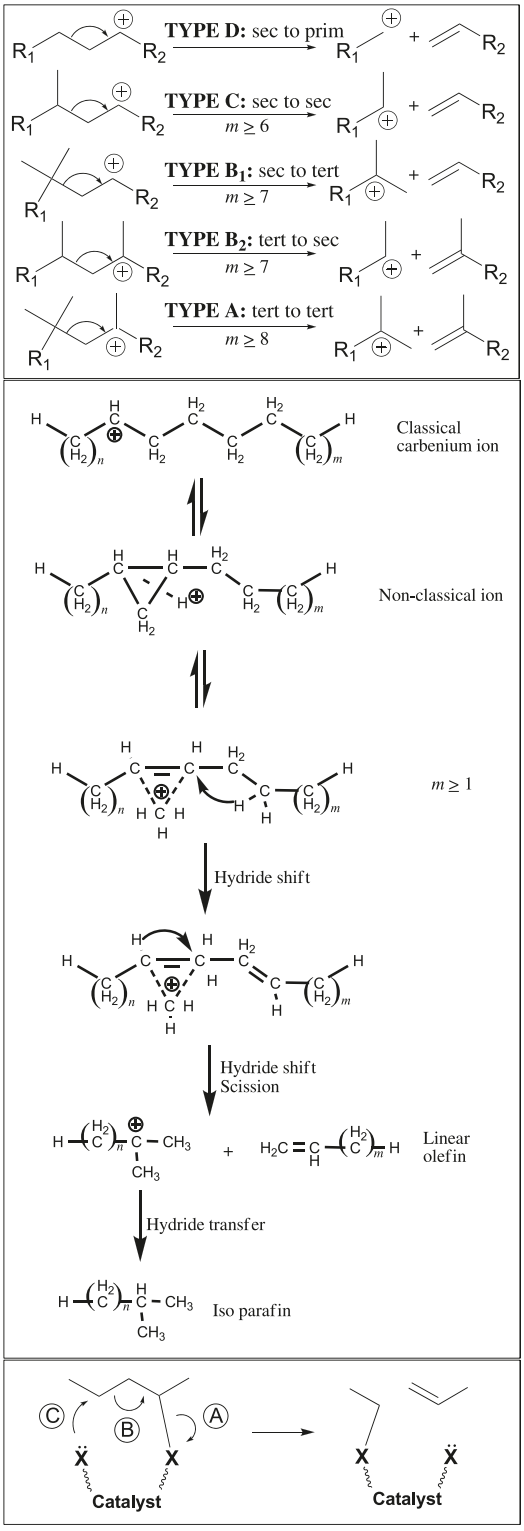

primary carbocations by requiring *n*-alkyl ions to undergo skeletal branching first, so that β scission could begin with secondary or tertiary ions and lead directly to secondary or tertiary ions. Their scheme categorized the reactions by ion type, and helped to explain the absence of two-carbon fragments in cracking experiments. Although the classical mechanism for skeletal branching was also at odds with the primary carbocation dilemma, by 1983 there was a newer branching mechanism proposed by others that involved a nonclassical protonated cyclopropane (PCP$^+$) structure (see the Discussion section).

In 1992–1993, Sie published a series of three papers,[6–8] which criticized the WJM[5] classical scheme, suggesting that if PCP$^+$ structures exist for the branching step, then they should exist for the β scission step as well. The mechanism of the 1992 Sie paper[6] is the most detailed (Fig. 1, middle), with hydrogen–atom rearrangement steps, and features the product double bond forming outside of the PCP$^+$ structure. Far less steps are presented in the 1993 papers.[7,8] The Sie[6–8] mechanism has been quoted often.[3,4,9]

The third prominent variation has been the chemisorption hypothesis, put forward by Kazansky and Senchenya[10] and popularized by van Santen and co-workers.[11] In this hypothesis, the carbocations are thought to exist not as classical or nonclassical ions, but as alkyl substituents chemisorbed to the catalyst (typically an oxygen atom in an aluminosilicate zeolite). Such alkoxide or silyl-ether structures are the only forms of nonresonant alkyl ions observed in in situ NMR experiments.[12] This variation can avoid the primary carbocation dilemma because, shortly after desorption, β scission can proceed as an S_N2 reaction (Fig. 1, bottom): instead of β scission resulting in a primary alkyl fragment containing the gamma carbon atom, a nucleophilic site on the catalyst attacks the gamma carbon first, causing the β scission while preventing the formation of a primary alkyl fragment.

In the first two papers of this series,[13,14] we examined this third variation, because we recognized that all previous computational studies[15] were adversely affected by the computational expense required to calculate transition states correctly, and hence made unfortunate compromises. Our work entailed computational geometry-optimization studies of secondary carbenium ions ($C_5H_{11}^+$, $C_6H_{13}^+$) on aluminum-containing molecular fragments of varying sizes, thoroughly exploring the potential energy surfaces and using accurate transition-state algorithms. One of the major conclusions was that the mechanism tended to be two-step, with the initial step being desorption and the rate-limiting second step being S_N2 β scission. This conclusion opens the possibility that desorption might lead to the Sie[6–8] or WJM[5] mechanisms, instead of the S_N2 second step of the chemisorption mechanism.

Faced with multiple possibilities, we have switched tactics and turned to rising-temperature molecular dynamics (MD) simulations[16] based on PW91 density functional theory. The simulation should, in principle, reveal which of the three β-scission variations is most likely to occur. Use of ab initio MD simulation to explore mechanisms was promoted by Dupuis and co-workers.[17] The rising-temperature technique is a means of increasing the probability of observing a chemical "rare event" in the narrow molecular times of the simulation (typically 10 ps from a week of simulation).

Fig. 2. Octyl ions studied.

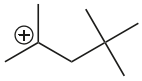

2,4,4-trimethylpent-2-yl cation

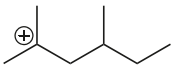

2,4-dimethylhex-2-yl cation

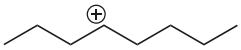

oct-4-yl cation

Although the simulated temperatures did get artificially high (sometimes over 2000 K), potentially opening up alternative high-barrier reaction possibilities, the processes with lower barriers remain orders of magnitude more probable. Furthermore, our simulations are incapable of producing homolytic C–C bond cleavage, because all electrons are required to be paired and hence unable to create radical products.

In this paper, we report the results of several simulations: five of *sec*-*n*-nonyl in the ionic liquid, $[(C_5H_5NH^+)_5(Al_2Cl_7^-)_6]^-$,[18] fifteen of *sec*-*n*-heptyl in chabazite, $[AlSi_{23}O_{48}]^-$,[19] two of *sec*-*n*-heptyl in chabazite, $[Al_4Si_{20}O_{45}(OH)_3]^-$, and a set of six from combining each of three octyl ion isomers (Fig. 2) with each of the first two catalysts. This final set of six include branched isomers to better test the WJM[5] mechanism. The ionic liquid simulations were motivated by the experiments of Johnson and co-workers,[18] who demonstrated that this particular liquid could crack nonane.

Methods

The ab initio molecular dynamics (AIMD) simulations were performed with the Vienna ab initio simulation package (VASP).[20] The level of theory was PW91, a gradient-corrected density functional theory (GGA DFT).[21] The calculations used Blöchl's[22] projector augmented wave technique,[23] applied to pseudopotentials appropriate for GGA DFT,[24,25] and a plane-wave basis set with various choices of the energy cutoff parameter ENMAX (350–500 eV). Simulations were performed with the NVT (canonical) ensemble, using a Nosé[26] thermostat set for a thermal oscillation every 40 timesteps (SMASS = 0), and a Verlet velocity algorithm[27] with a timestep of 1 fs. These condensed-phase calculations employed periodic replication of a unit cell, and calculations were restricted to the gamma point. The unit cell contained catalysts of an overall –1 charge, to counterbalance the positive charge of the alkyl ion. Each atom had an isotope-averaged mass (e.g., 35.453 amu for Cl), except for H (mass 1.000 amu).

Simulations were performed of various C_7–C_9 alkyl ions in three different condensed-phase catalytic environments (Fig. 3). System IL was an ionic liquid, consisting of five pyridinium cations ($C_5H_5NH^+$) and six $Al_2Cl_7^-$ ions. Sys-

Fig. 3. Snapshot of parent geometries (within the replicated cell) used for simulations. Atom colour scheme: C atoms of alkyl ion, light blue; C atoms of pyridinium ions, light grey; N atoms of pyridinium ions, dark blue; Cl atoms, green; H atoms, white; O atoms, red; Si atoms, dark grey; Al atoms, pink.

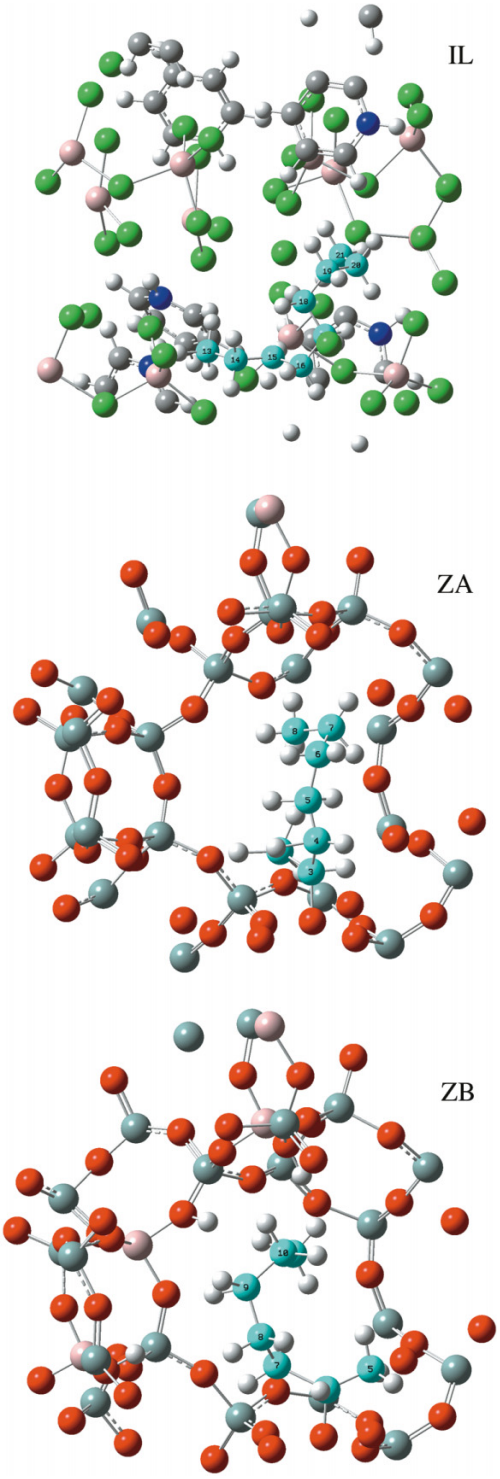

tems ZA and ZB were based on chabazite zeolite; our unit cell contains $Si_{24}O_{48}$ (twice the true unit cell of chabazite). System ZA had an Al^- substituted in the place of one Si atom. System ZB was derived from system ZA by the sub-

Fig. 4. Energy (upper plot) and temperature (lower plot) vs. time for the 50 K quench run of trimethylpentyl ion on chabazite ZA. E_0: potential energy for nuclear motion. $E_0 + E_K$: total internal energy. Regular nuclear speeds (temperature plot) are achieved after ~50 fs.

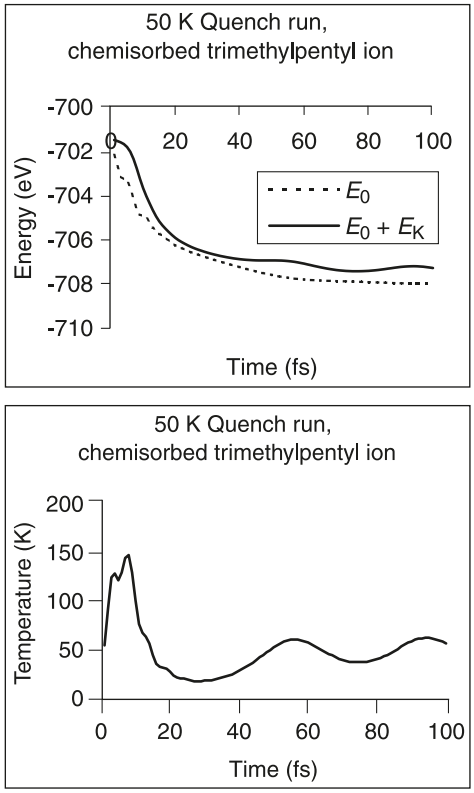

stitution of three Si–O diatom units with Al–O–H units. The purpose of system ZB was to increase the number of Brønsted acid sites, because simulations with system ZA tended to quickly result in deactivation of the carbocation to an alkene, thereby requiring reactivation by a Brønsted site. Details on the initial structures can be found in Appendices A–C.

Results

Preparatory runs

Equilibration runs were performed as described in Appendices A–C. For the zeolite simulations, attempts at equilibrating chemisorbed alkyl ions normally resulted in immediate desorption. We present some results from our preparatory runs to reassure the reader that we did ensure that immediate desorption was not the result of poor initial geometries.

For the tertiary 2,4,4-trimethylpent-2-yl ion, in system ZA, a quick quench run was performed at 50 K for only 100 fs. The choice of initial chemisorbed structure did not produce unreasonable velocities at the start (Fig. 4), but desorption began regardless, after only one C–O vibrational period (Fig. 5). Hence, one cannot equilibrate tertiary carbocations chemisorbed to chabazite with PW91-based simulations.

For *n*-alkyl secondary ions, which should bind more strongly than tertiary ions, we could maintain chemisorption at temperatures below ~1000 K, but above 1000 K desorption would occur within 1 ps. For instance, when our simulation of *n*-4-octyl chemisorbed on system ZA showed rapid desorption upon simulation above 1000 K, we tried a 4000 fs chemisorption-maintaining pseudo-equilibration run, rising in temperature from 200 to 600 K, before relaunching the production run from 1000 K. This relaunched production run produced desorption at t = 50 fs, earlier than in the original, nonequilibrated run (Fig. 5).

Fig. 5. Plot of chemisorption bond lengths to chabazite ZA vs. time: an equilibrated run (dashed line), a pre-equilibrated run (thick line), and the 50 K quench run for the tertiary trimethylpentyl ion (black line), demonstrating rapid desorption in each case.

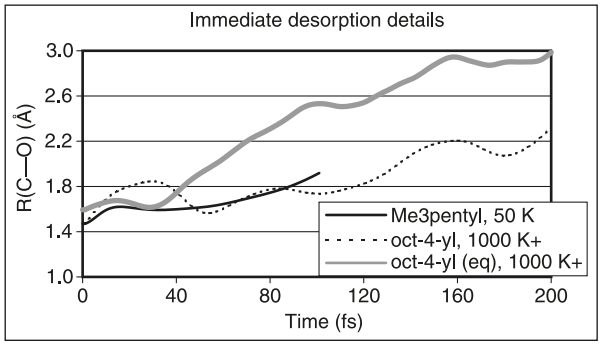

Production runs: unbranched alkyl ions

Twenty four of our 28 production runs began with *sec-n*-alkyl ions: six with desorbed ions in ionic liquid (IL) (Table 1, run 1, and Table 2) and 18 with chemisorbed ions on chabazite systems ZA and ZB (Tables 3 and 4, and Table 1, run 2). Of these 24 runs, β scission was observed in only the very first one: the ion branched first[17] and then, after taken to a very high temperature, performed a very rare tertiary-to-primary β scission. Although the other 23 runs did not produce β scission, there is useful information to be gleaned from them. One general observation from these other 23 runs was that the ultimate fate of the ions was deactivation: the loss of H^+ back to the catalyst to generate an alkene. On longer timescales, these C_7–C_9 alkenes could be reactivated by the Brønsted catalyst, but such a reactivation was not observed in the small (10^{-11} s) timescales of the simulations, even in system ZB, presumably because reactivation is a neutral–neutral bimolecular reaction requiring a specific low-probability collision.

Of the six runs in system IL, three resulted in branching before deactivation occurred. Several 1,2-H-shifts were observed, as were episodes of short-lived (~100 fs) PCP^+ structures, particularly at temperatures above 1000 K. Secondary carbocations tended to live for 1–4 ps in these rising-temperature simulations, until temperatures reached 1800–2000 K. Branching occurred between 1300 and 2000 K, after which the tertiary carbocations tended to live another 1–4 ps, until temperatures reached ~2500 K. The stability of these ions in system IL at constant temperatures was not tested: at experimental temperatures (~373 K) these ions would be expected to live longer, although not indefinitely, as carbocations would undergo oligomerization and cracking cycles until they either reach their most stable form (*t*-butyl ions) or become deactivated hydrocarbons that would settle into an organic layer.

Table 1. The results of simulations of various octyl ions.

Run	Baseline temperature (K)	Time (fs)	Event description
1. Oct-4-yl cation, system IL	1000 + 0.25/fs (to 2000)	1225	1,2-Propyl-shift, sec → prim
		1250	1,3-H-shift, prim → sec
		1695	1,2-Methyl-shift, sec → sec
		3590	1,2-H-shift, sec → prim
		3650	1,2-Hexyl-shift, prim → prim
		3730	1,6 H-shift (ene + pentavalent C)
		3830	Loss of H_2 (3-methylhept-6-en-2-yl)
		4010	Deactivation
2. Oct-4-yl cation, system ZA	1000 + 0.25/fs (to 2000)	135	Desorption
		3045	Deactivation
3. 2,4-Dimethylhex-2-yl cation, system IL	1000 + 0.25/fs (to 2000)	2250	1,2-H-shift, tert → sec
		2380	1,2-H-shift, sec → tert
		2790	1,2-H-shift, tert → sec
		2850	1,2-Ethyl-shift, sec → sec
		3468	***β Scission, sec → sec***
		3858	Deactivation
4. 2,4-Dimethylhex-2-yl cation, system ZA	1000 + 0.25/fs (to 2000)	20	Desorption
		365–546	Attempted β scission
		875–1005	Attempted β scission
		1905	***β Scission, tert → sec***
		3735	H transfer, sec → tert
5. 2,4,4-Trimethylpent-2-yl cation, system IL	600 + 0.2/fs (to 2200)	6880	***β Scission, tert → tert***
		7060	Deactivation
6. 2,4,4-Trimethylpent-2-yl cation, system ZA	300 + 0.25/fs (to 1300)	1	Desorption
		2317	***β Scission, tert → tert***
		3000	H transfer, tert → tert

Note: In each run, ENMAX = 350 eV. Deactivation refers to the loss of H^+ to the catalyst. H transfer refers to the transfer between hydrocarbon fragments. The numerous 1,2-H-shifts that did not result in a change of ion type were not reported.

Table 2. The results of simulations of non-3-yl ion in system IL (ionic liquid).

Run	Baseline temperature (K)	Time (fs)	Event description[a]
1	973 + 0.2/fs	5000	Branched, sec → tert
		7705	***β Scission, tert → prim***
		7775	Deactivated
2	973 + 0.2/fs	4248	Deactivated
3	1773 + 0.1/fs	145	Branched, sec → tert
		5583	Deactivated
4	1773 + 0.2/fs	1630	Deactivated
5	1773 + 0.2/fs	1380	Deactivated

Note: Each run was continued until deactivation occurred, and ENMAX = 400 eV except for runs 1 and 5 (500 eV).

[a]At these elevated temperatures, H-shifts were too numerous to report.

The 18 runs with the model zeolite systems, ZA and ZB, were begun with the alkyl ions in the chemisorbed state, to test the chemisorption hypothesis (Fig. 1), but the ion either stayed chemisorbed (three runs) or desorbed without performing the S_N2 β scission step (15 runs). Deactivation generally occurred at lower temperatures (1000–1800 K) than with the ionic liquid catalyst (>1700 K), because the zeolite is a stronger conjugate base than the ionic liquid, and this early deactivation is likely why neither cracking nor branching was observed in any of these 18 runs. In Table 3, several constant-temperature runs were performed to lengthen times before deactivation, but these longer times were not long enough to witness any branching or β scission events. The longest lifetime observed for a desorbed alkyl ion inside chabazite was 4.7 ps (Table 3, runs 3e and 4a).

Production runs: branched alkyl ions

In contrast to the 24 *sec-n*-alkyl runs, all four of the branched-alkyl runs succeeded in performing β scission, and are reported as the last four runs of Table 1. We make some minor remarks first. In Table 1, run 3, the starting tertiary ion spent some time as a secondary ion, during which an ethyl shift occurred before the β scission event. In Table 1, run 4 there were two unsuccessful attempts at β scission before the successful one occurred; this is demonstrated in Fig. 6 as a plot of the β C–C bond distance vs. time. In Table 1, runs 4 and 6, there were hydrogen transfers between the two product fragments, after β scission, the probability of which was likely enhanced by the solid pore structure of the zeolite, which kept the two fragments in close proximity.

Most importantly, in all four cases, the β scission mechanisms observed were classical WJM[5] ones from desorbed ions. No attempts at chemisorption-style S_N2 β scission were observed. Although occasional PCP^+ structures were observed for secondary alkyl ions during the simulations, none existed during the β scission events: in Fig. 7 we plot the critical C–C–C angle during the C–C bond scission events in these four runs, and the angle is never near the $\sim 80^\circ$ expected for a PCP^+ structure. The observed β-scission reactions are summarized in Table 5.

Table 3. The results of simulations of chemisorbed hept-2-yl ion in system ZA (zeolite).

Run	Baseline temperature (K)	Event description
Set I		
1	298	Stayed chemisorbed
2	300 + 0.2/fs (to 1100)	Stayed chemisorbed
3 (from 2)	1100 + 0.2/fs	Desorbed 770 fs, 3,2-H-shift 1600 fs, deactivated 1990 fs
3b (from 2)	1100 + 0.2/fs	Desorbed 50 fs, deactivated 500 fs
3c (from 2)	1000	Stayed chemisorbed
Set II (from 3c)		
3d[a]	1000	Desorbed 535 fs, deactivated 1670 fs
3f[a]	1100	Desorbed 500 fs, 3,2-H-shift 2035 fs, 2,3-H-shift 2065 fs, deactivated 2790 fs, reactivated 2920 fs, 3,2-H-shift 2935 fs, re-chemisorbed 3320 fs
3g[a]	1200	Desorbed 510 fs, 3,2-H-shift 1110 fs, 4,3-H-shift 1375 fs, deactivated 1465 fs
3e[a]	1300	Desorbed 500 fs, 3,2-H-shift 1220 fs, 5,3-H-shift 2340 fs, 6,5-H-shift 3440 fs
Set III (from 3c)		
4d[b]	1000	Desorbed 3150 fs, deactivated 3340 fs
4f[b]	1100	Desorbed 1200 fs, deactivated 1630 fs
4g[b]	1200	Desorbed 2080 fs, deactivated 2200 fs
4e[b]	1300	Desorbed 430 fs, deactivated 660 fs
Set IV (from 3e)		
4a[c]	1300	Deactivated 1250 fs
4b[d]	1300	Deactivated 2170 fs

Note: In each run, ENMAX = 350 eV and the length of the runs were 4000 fs.
[a]Set II runs began with the last positions and velocities of run 3c.
[b]Set III runs began with the last positions of run 3c, but with fresh Boltzmann velocities each run.
[c]Run 4a began with the last positions and velocities of run 3e.
[d]Run 4b began with the last positions of run 3e, but with fresh Boltzmann velocities.

Table 4. Results of simulations of chemisorbed hept-2-yl ion in system ZB (zeolite).

Run	Baseline temperature (K)	Length of simulation (fs)	Event description
1	1500	12000	Desorbed 140 fs, 3,2-H-shift 510 fs, deactivated 520 fs
1b	1900	4000	Desorbed 120 fs, 1,2-H-shift 250 fs, deactivated 267 fs, reactivated 285 fs, deactivated 380 fs

Note: In each run, ENMAX = 350 eV.

Fig. 6. A plot of the rupturing C–C bond distance vs. time, Table 1, run 4 (dimethylhexyl ion, chabazite catalyst).

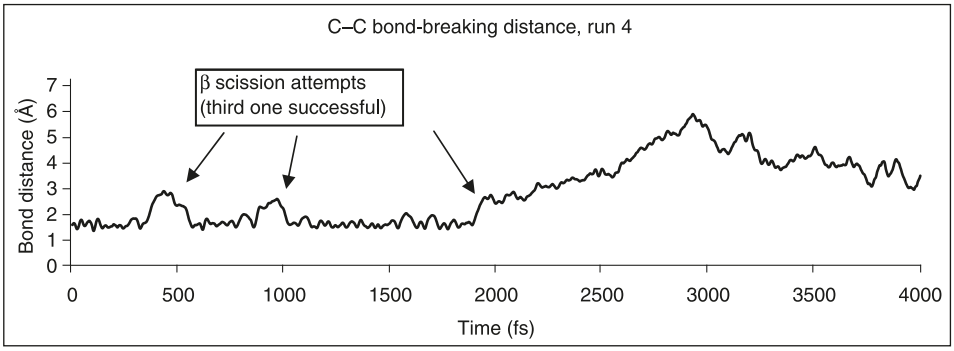

The use of artificially high temperatures does not bias the simulations against producing PCP^+ structures and Sie's[6–8] nonclassical mechanism; in fact, it produces more of these high-energy structures, but no β scissions resulted from them. The use of artificially high temperatures may bias the simulations against the chemisorption hypothesis, if it promotes desorption over S_N2 reaction, but our previous potential-energy-surface work[13,14] has already indicated that partial desorption is a commonly required step even at 0 K. Indeed, all the simulations are in accord with the WJM[5] scheme, in which desorbed and branched classical carbocations are the ones that undergo β scission.

Discussion

PCP^+ as an intermediate in *isomerizations* was proposed long ago, perhaps first by Nevell, de Salas, and Wilson,[28] who in 1939 described the possibility of an intermediate

Fig. 7. $C^+–C_\alpha–C_\beta$ bond angles during the four β scission events of Table 1. An expected angle for a β scission from a PCP^+ intermediate would be 80°, which was not observed.

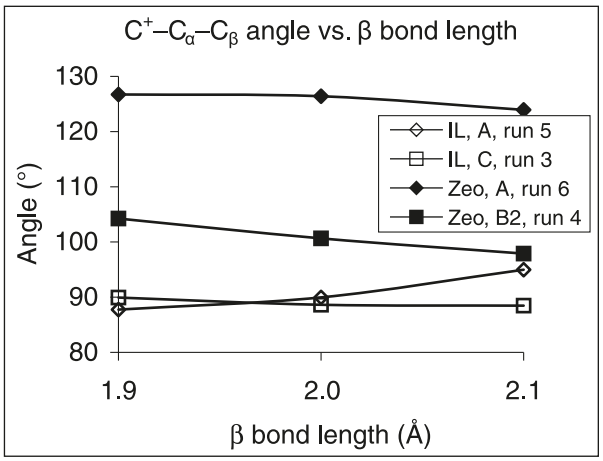

"mesomeric" between the two classical carbocation intermediates that Meerwein and van Emster[29] had postulated for the Wagner–Meerwein rearrangement. In the Wagner–Meerwein rearrangement, the PCP^+ ring has four alkyl substituents (2,1,1 distribution). In 1943, in a general article on organic reaction rates, Eyring, Hulbert, and Harman[30] speculated that "triangular configurations" for carbocations should have low enough energies to explain 1,2-alkyl rearrangements, quoting the early calculations on H_3^+ by Hirschfelder,[31] which revealed a triangular minimum-energy structure. These two suggestions, plus knowledge of triangular Ag^+-bridged alkenes,[32] led Winstein and Trifan[33] in 1949 to draw a symmetric "alkyl-bridged" norbornyl carbocation intermediate to account for racemization of its substituted exo enantiomers. In this racemization, the PCP^+ ring has only three substituents (1,1,1 distribution). Brown[34] would later famously contest the symmetric PCP^+ structure in Winstein and Trifan's[33] case, arguing that it is a transition state but not an intermediate. However, quantum chemistry calculations since 1983[35,36] have demonstrated that the bare ion does indeed have the (symmetric) PCP^+ structure, and not a classical one as Meerwein[29] would have thought.

In the Wagner–Meerwein and norbornyl rearrangements, the three participating carbons in the PCP^+ ring are tethered in a tricyclic structure. In 1952, Stevenson et al.[37] extended the PCP^+ idea for acyclic alkyl ions, proposing such structures as intermediates for alkyl shifts that change the amount of branching in the ion. This required a 1,2-H-shift to take place "concomitantly" with the PCP^+ branching mechanism. McCaulay,[38] in 1959, published a rate study demonstrating much slower rates of rearrangements for those that change the extent of branching, and explained this with PCP^+ arguments, arguing that PCP^+ allows partial, but not complete, avoidance of primary carbenium ion structures in the branching cases. The role of the hydrogens during branching was correctly postulated by Edwards and Lesage[39] in 1963, with the mechanism determined to be two-step in 1996 calculations by Corma and co-workers[40] and verified in recent simulations.[17] A seminal demonstration of the importance of PCP^+ structures for nontethered alkyl ions was provided by the thorough ab initio study of $C_4H_9^+$ conformers by Sieber et al.[41]

Table 5. Summary of β-scission events observed in our simulations.

Type	Reaction	Catalyst system
tert→tert (A)	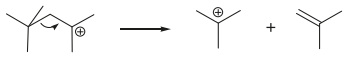	Ionic liquid Zeolite
tert→sec (B_2)	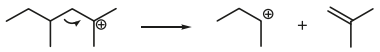	Zeolite
sec→sec (C)	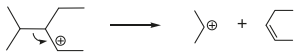	Ionic liquid
tert→prim	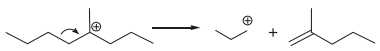	Ionic liquid

In contrast, there is no such long history of PCP^+ as an intermediate in *β scission*. Sie[6] proposed this mechanism in 1992. We could not find any significant challenges to this proposal in the literature, but there are in fact three criticisms that can be made. First, the Sie[6–8] mechanism is faulty on theoretical grounds because, in the last structure leading to β scission (Fig. 1, middle panel, fourth structure down), there are two carbon atoms each sharing 10 electrons (third and fourth carbons from the right), a disastrous violation of the octet rule. Second, this mechanism describes not β scission, but γ scission, and is thus clearly contrary to experimental evidence. Third, Sie[6–8] had originally criticized the WJM[5] mechanism because it implied that cracking rates should be independent of the original extent of branching (WJM[5] assumed that branching occurs before cracking), in contrast to experiments such as those by Nace,[42] which appeared to show otherwise. However, the Nace[42] experiments that Sie[6–8] quoted were two-minute experiments on alkanes with a zeolite catalyst, and can be explained (as Nace[42] himself did) by realizing that the overall cracking rate is determined by the initiation step, not the branching or cracking steps. The two probable reasons why Nace's[42] heptamethylnonane cracked more slowly than *n*-hexadecane are that (*i*) each heptamethylnonane molecule had only seven attackable hydrogens (six secondary and one tertiary), while each *n*-hexadecane has 28 (all secondary), and (*ii*) the heptamethylnonane possessed three quaternary carbon atoms, giving the molecule sufficient bulk that it may have had difficulty fitting into the zeolite pores.

Since the current study demonstrates that simulations biased towards PCP^+ structures (due to elevated temperatures) do not use PCP^+ structures during β scission, it would seem appropriate to retire the Sie[6–8] mechanism altogether. Since the WJM[5] mechanism only applies to hexyl ions and larger, there may be a role for PCP^+ structures in the extreme high-temperature monomolecular cracking of pentyl and butyl ions, but certainly not with 10-valence-electron carbon atoms as Sie[6] had envisaged.

The chemisorption hypothesis, while unimportant for ionic liquids, cannot yet be ruled out for zeolites. The simulations employed here used elevated temperatures, which are biased toward desorption. There might also be possible bias against the chemisorption hypothesis due to the PW91 DFT approximation, which might underestimate desorption ener-

gies and overestimate S_N2-scission barriers due to omission of dispersion interactions; future research should test these possibilities. However, since computed activation enthalpy barriers[13,14] for the chemisorption mechanism are not much lower than those for full desorption, since entropy would favour desorption, and since our simulations gave four instances of unimolecular scission and none of bimolecular-S_N2 scission, it would seem to us that the S_N2-chemisorbed mechanism in Fig. 1 is on shakier ground than unimolecular WJM[5] mechanisms. We are now inclined to think that the chemisorbed state is a storage state for alkyl ions, but that β scission likely occurs in the desorbed state. Although in situ NMR experiments have failed to identify desorbed carbocations inside zeolites, the simulations offer the explanation that the desorbed alkyl ions simply have short (10^{-9} to 10^{-12} s) lifetimes relative to deactivation to alkenes (or chemisorption), and that cracking must occur during these brief but periodic lifetimes.

Conclusions

In 28 simulations of branched and unbranched alkyl (carbenium) carbocations in the presence of catalysts, only the branched alkyl ions performed β scission within simulation timescales, and all five performed straightforward bond breaking without involving chemisorbed or PCP^+ structures. Formation of a primary carbocation, which would have been produced by β scission of *sec-n*-alkyl ions, is simply not energetically favourable, and only occurred in one simulation at a very high temperature (>2500 K). Desorption was common to all simulations that began in the chemisorbed state, and the lifetimes of desorbed carbocations (relative to deprotonation by the zeolite) was <5 ps at 1000–2000 K. These new simulations give support for the WJM[5] classical mechanism, and not for the Sie[6–8] PCP^+ mechanism, which has several theoretical problems. The S_N2-chemisorbed and alternative PCP^+ mechanisms cannot yet be ruled out, but they should be considered targets for further scrutiny.

Acknowledgements

Grants were made available by the Natural Sciences and Engineering Research Council of Canada (NSERC) and the Canada Foundation for Innovation (CFI). All simulations were performed on a Parallel Quantum Solutions computer (56 processors) housed in the Laboratory of Computational Discovery at the University of Regina. J. Hafner and T. Bučko (University of Vienna) are thanked for for valuable advice, and T. Bučko for providing the chabazite input deck.

References

(1) Thomas, C. L. *Ind. Eng. Chem.* **1949**, *41* (11), 2564–2573. doi:10.1021/ie50479a042.

(2) Greensfelder, B. S.; Voge, H. H.; Good, G. M. *Ind. Eng. Chem.* **1949**, *41* (11), 2573–2584. doi:10.1021/ie50479a043.

(3) Kissin, Y. V. *Catal. Rev.* **2001**, *43* (1–2), 85–146. doi:10.1081/CR-100104387.

(4) Akhmedov, V. M.; Al-Khowaiter, S. H. *Catal. Rev.* **2007**, *49* (1), 33–139. doi:10.1080/01614940601128427.

(5) Weitkamp, J.; Jacobs, P.; Martens, J. A. *Appl. Catal.* **1983**, *8* (1), 123–141. doi:10.1016/0166-9834(83)80058-X.

(6) Sie, S. T. *Ind. Eng. Chem. Res.* **1992**, *31* (8), 1881–1889. doi:10.1021/ie00008a008.

(7) Sie, S. T. *Ind. Eng. Chem. Res.* **1993**, *32* (3), 397–402. doi:10.1021/ie00015a001.

(8) Sie, S. T. *Ind. Eng. Chem. Res.* **1993**, *32* (3), 403–408. doi:10.1021/ie00015a002.

(9) (a) Jentoft, F. C.; Gates, B. C. *Top. Catal.* **1997**, *4* (1/2), 1–13. doi:10.1023/A:1019184004885.; (b) Ono, Y. *Catal. Today* **2003**, *81* (1), 3–16. doi:10.1016/S0920-5861(03)00097-X.; (c) Leckel, D. *Energy Fuels* **2007**, *21* (3), 1425–1431. doi:10.1021/ef060601x.; (d) Bhan, A.; Gounder, R.; Macht, J.; Iglesia, E. *J. Catal.* **2008**, *253* (1), 221–224. doi:10.1016/j.jcat.2007.11.003.

(10) Kazansky, V. B.; Senchenya, I. N. *J. Catal.* **1989**, *119* (1), 108–120. doi:10.1016/0021-9517(89)90139-5.

(11) (a) Bates, S. P.; van Santen, R. A. *Adv. Catal.* **1998**, *42*, 1–114. doi:10.1016/S0360-0564(08)60627-6.; (b) Frash, M. V.; van Santen, R. A. *Top. Catal.* **1999**, *9* (3/4), 191–205. doi:10.1023/A:1019183110705.

(12) (a) Nicholas, J. B.; Haw, J. F. *J. Am. Chem. Soc.* **1998**, *120* (45), 11804–11805. doi:10.1021/ja982012e.; (b) Haw, J. F. *Phys. Chem. Chem. Phys.* **2002**, *4* (22), 5431–5441. doi:10.1039/b206483a.

(13) Li, Q.; East, A. L. L. *Can. J. Chem.* **2005**, *83* (8), 1146–1157. doi:10.1139/v05-135.

(14) Li, Q.; East, A. L. L. *Can. J. Chem.* **2006**, *84* (9), 1159–1166. doi:10.1139/V06-143.

(15) (a) Frash, M. V.; Kazansky, V. B.; Rigby, A. M.; van Santen, R. A. *J. Phys. Chem. B* **1998**, *102* (12), 2232–2238. doi:10.1021/jp973203r.; (b) Hay, P. J.; Redondo, A.; Guo, Y. *Catal. Today* **1999**, *50* (3–4), 517–523. doi:10.1016/S0920-5861(98)00486-6.; (c) Svelle, S.; Kolboe, S.; Swang, O. *J. Phys. Chem. B* **2004**, *108* (9), 2953–2962. doi:10.1021/jp0371985.; (d) Demuth, T.; Rozanska, X.; Benco, L.; Hafner, J.; van Santen, R. A.; Toulhoat, H. *J. Catal.* **2003**, *214* (1), 68–77. doi:10.1016/S0021-9517(02)00074-X.

(16) (a) Sørensen, M. R.; Voter, A. F. *J. Chem. Phys.* **2000**, *112* (21), 9599–9606 doi:10.1063/1.481576.; (b) East, A. L. L.; Bučko, T.; Hafner, J. *J. Phys. Chem. A* **2007**, *111* (27), 5945–5947. doi:10.1021/jp072327t. PMID:17559202.

(17) Ammal, S. C.; Yamataka, H.; Aida, M.; Dupuis, M. *Science* **2003**, *299* (5612), 1555–1557. doi:10.1126/science.1079491. PMID:12624261.

(18) Xiao, L.; Johnson, K. E.; Treble, R. G. *J. Mol. Catal. A* **2004**, *214* (1), 121–127. doi:10.1016/j.molcata.2003.12.030.

(19) Bučko, T.; Benco, L.; Hafner, J.; Ángyán, J. G. *J. Catal.* **2007**, *250* (1), 171–183. doi:10.1016/j.jcat.2007.05.025.

(20) Kresse, G.; Furthmüller, J. *J. Phys. Rev. B* **1996**, *54* (16), 11169–11186. doi:10.1103/PhysRevB.54.11169.

(21) Perdew, J. P.; Chevary, J. A.; Vosko, S. H.; Jackson, K. A.; Pederson, M. R.; Singh, D. J.; Fiolhais, C. *Phys. Rev. B* **1992**, *46* (11), 6671–6687. doi:10.1103/PhysRevB.46.6671.

(22) Blöchl, P. E. *Phys. Rev. B* **1994**, *50* (24), 17953–17979. doi:10.1103/PhysRevB.50.17953.

(23) Kresse, G.; Joubert, D. *Phys. Rev. B* **1999**, *59* (3), 1758–1775. doi:10.1103/PhysRevB.59.1758.

(24) Vanderbilt, D. *Phys. Rev. B* **1990**, *41* (11), 7892–7895. doi:10.1103/PhysRevB.41.7892.

(25) Kresse, G.; Hafner, J. *J. Phys. Condens. Matter* **1994**, *6* (40), 8245–8257. doi:10.1088/0953-8984/6/40/015.

(26) Nosé, S. *J. Chem. Phys.* **1984**, *81* (1), 511–519. doi:10.1063/1.447334.

(27) Allen, M. P.; Tildesley, D. J. *Computer Simulations of Liquids;* Clarendon: Oxford, UK, 1987.

(28) Nevell, T. P.; de Salas, E.; Wilson, C. L. *J. Chem. Soc.* **1939**, 1188. doi:10.1039/jr9390001188.
(29) Meerwein, H.; van Emster, K. *Chem. Ber.* **1922**, *55*, 2500–2528.
(30) Eyring, H.; Hulburt, H. M.; Harman, R. A. *Ind. Eng. Chem.* **1943**, *35* (5), 511–521. doi:10.1021/ie50401a003.
(31) Hirschfelder, J. O. *J. Chem. Phys.* **1938**, *6* (12), 795–806. doi:10.1063/1.1750173.
(32) Winstein, S.; Lucas, H. J. *J. Am. Chem. Soc.* **1938**, *60* (4), 836–847. doi:10.1021/ja01271a021.
(33) Winstein, S.; Trifan, D. S. *J. Am. Chem. Soc.* **1949**, *71* (8), 2953. doi:10.1021/ja01176a536.
(34) Brown, H. C. *The Nonclassical Ion Problem;* Plenum Press: New York, 1977.
(35) Raghavachari, K.; Haddon, R. C.; Schleyer, P. R.; Schaefer, H. F., III. *J. Am. Chem. Soc.* **1983**, *105* (18), 5915–5917. doi:10.1021/ja00356a034.
(36) Yoshimine, M.; McLean, A. D.; Liu, B.; DeFrees, D. J.; Binkley, J. S. *J. Am. Chem. Soc.* **1983**, *105* (19), 6185–6186. doi:10.1021/ja00357a055.
(37) Stevenson, D. P.; Wagner, C. D.; Beeck, O.; Otvos, J. W. *J. Am. Chem. Soc.* **1952**, *74* (13), 3269–3282. doi:10.1021/ja01133a017.
(38) McCaulay, D. A. *J. Am. Chem. Soc.* **1959**, *81* (24), 6437–6443. doi:10.1021/ja01533a026.
(39) Edwards, O. E.; Lesage, M. *Can. J. Chem.* **1963**, *41* (6), 1592–1605. doi:10.1139/v63-218.
(40) Boronat, M.; Viruela, P.; Corma, A. *J. Phys. Chem.* **1996**, *100* (41), 16514–16521. doi:10.1021/jp961179w.
(41) Sieber, S.; Buzek, P.; Schleyer, P. R.; Koch, W.; Carneiro, J. W. M. *J. Am. Chem. Soc.* **1993**, *115* (1), 259–270. doi:10.1021/ja00054a037.
(42) Nace, D. M. *Ind. Eng. Chem. Prod. Res. Dev.* **1969**, *8* (1), 31–38. doi:10.1021/i360029a005.

Appendix A. Starting geometries: system IL

An ionic liquid starting geometry was meticulously built by hand, with six $[C_5H_5NH]^+$ ions and six $[Al_2Cl_7]^-$ ions, in a cubic unit cell of width 13.72 Å to match the experimental density of 1.476 g/mL.[18] This was equilibrated at 373 K with a Nosé[26] thermostat for 1004 fs. Initially, the temperature rose to 1700 K due to the initial forces caused by the artificial geometry, but the thermostat quenched this within 50 fs, and the cell energy was steady from 200 fs onward. The velocities of all 126 atoms were plotted vs. time to ensure that no lingering "hot modes" existed after 1004 fs.

Table 2 runs: the structure from the first equilibration was taken, the cell width was expanded from 13.72 to 13.90 Å (a 4% volume expansion), and one $C_5H_5NH^+$ was replaced with a non-3-yl ion (Fig. 3, top). This corresponds to a nonyl ion concentration of 5% by weight; although the experiment of interest[18] used 25% nonane by weight, the nonane is insoluble in an ionic liquid until it is ionized, so that 5% nonyl ion concentration may be a reasonable estimate of reality. Four copies of this geometry file were made. The first copy was further equilibrated, for 3000 fs at 773 K followed by another 3000 fs at 973 K, and then split into two copies for trials 1 and 2, each starting at 973 K. Trials 3, 4, and 5 ignored the further 6 ps of equilibration and began from the three other original copies.

Table 1 runs: the structure from the first equilibration was taken, the cell width was expanded from 13.72 to 13.90 Å (a 4% volume expansion), one $C_5H_5NH^+$ was replaced with a 2,6-H-bridged $C_9H_{19}^+$ ion (originally intended for a different study), and this mixture was further equilibrated at 300 K for another 1000 fs (the $C_9H_{19}^+$ ion began and ended with the 2,6-H-bridge). The resulting structure was split into three copies, and in each the $C_9H_{19}^+$ ion was replaced with one of the three starting $C_8H_{17}^+$ ions of the current study. No further equilibration was performed, as the liquid quickly adjusted to the new ion in the first $\sim$100 fs of each of the rising-temperature runs in this study.

Appendix B. Starting geometries: system ZA

The chabazite structure, $[AlSi_{23}O_{48}]^-$, contains two unit cells of chabazite, with an Al atom substituted for a Si one, as described previously.[19] We received a pre-equilibrated one (containing a desorbed $C_4H_{11}^+$ ion) from Tomas Bučko (Vienna).

Table 3 runs: the desorbed $C_4H_{11}^+$ ion was replaced with a hept-2-yl ion chemisorbed to an oxygen atom neighbouring an Al atom of a replicated cell (Fig. 3, centre). The first run reported in Table 3 served as the equilibration run, but it possessed a continually rotating methyl group, so the second run was begun from the first but with velocities removed to reset the methyl rotation. All remaining runs in Table 3 are descendants of this second run.

Table 1 runs: the desorbed $C_4H_{11}^+$ ion was replaced with one of the three $C_8H_{17}^+$ ions of this study, chemisorbed to the same oxygen atom. Attempts at equilibrating the chemisorbed *sec*- and *tert*-alkyl ions failed to prevent immediate desorption (see text), so the rising-temperature production runs were run from the structures built.

Appendix C. Starting geometries: system ZB

Table 4 runs: the final heptyl ion/chabazite chemisorbed complex from run 3c of Table 3 was copied to a new input file, three Si atoms were replaced with Al atoms, and three H atoms were then added to O atoms bonded to these new Al atoms, creating three Brønsted AlOH sites within the same pore as the alkyl ion (Fig. 3, bottom). This structure was used as the starting structure for both runs in Table 4.